Room Temperature Direct and Heterodyne Detection of 0.28–0.69-THz Waves Based on GaN 2-DEG Unipolar Nanochannels

Carlos Daher, Jérémie Torres, Ignacio Iñiguez-de-la-Torre, Philippe Nouvel, Luca Varani, Paul Sangaré, Guillaume Ducournau, Christophe Gaquière, Javier Mateos, and Tomás González

Abstract—An experimental demonstration of GaN-based asymmetric nanodiodes as direct and heterodyne detectors up to 0.69 THz has been performed at room temperature. Responsivities of 2 and 0.3 V/W in a free-space configuration were obtained at 0.30 and 0.69 THz, respectively. An intermediate frequency (IF) signal has been measured up to 40 and 13 GHz in the same frequency ranges. The characterization of the nanodiodes as mixers did not show any deviation from linearity between the RF input power and the IF output. Monte Carlo simulations, used to estimate nanodevice intrinsic conversion losses of 27 dB at 0.69 THz, have confirmed these results.

Index Terms—Frequency conversion, microwave circuits, mixers, sensor systems and applications detectors semiconductor detectors.

I. INTRODUCTION

DIRECT detection, one of the possible homodyne methods, is based on detecting a frequency-modulated continuous-wave radiation by a nonlinear device, which is able to rectify an alternating current, and generating—as a result— a dc voltage. In practice, the detection is often realized using a square-wave reference the so-called switching-mode detection. This method is widely used in optical applications [1] and radio communications [2]. Synchronous detection enables

C. Daher, J. Torres, P. Nouvel, and L. Varani are with the Centre National de la Recherche Scientifique, Institut d'Electronique et des Systèmes, University of Montpellier, Montpellier 34090, France (e-mail: daher@ies.univ-montp2.fr; jeremi.torres@ies.univ-montp2.fr; nouvel@ies.univ-montp2.fr; luca.varani@univ-montp2.fr).

I. Iñiguez-de-la-Torre, J. Mateos, and T. González are with the Department of Applied Physics, University of Salamanca, Salamanca 37008, Spain (e-mail: indy@usal.es; javierm@usal.es; tomasg@usal.es).

P. Sangaré, G. Ducournau, and C. Gaquière are with the Institut d'Electronique, de Microlectronique et de Nanotechnologie, University of Lille 1, Lille F-59100, France (e-mail: pa.sangare@ed.univ-lille1.fr; guillaume.ducournau@iemn.univ-lille1.fr; christophe.gaquiere@iemn.univ-lille1.fr).

Color versions of one or more of the figures in this paper are available online at http://ieeexplore.ieee.org.

processing of very weak signals, even of amplitude lower than noise. It requires a reference signal with known frequency and phase, but it cannot give information about the frequency of the processed signal. An alternative method to detect a signal is the heterodyne detection by a nonlinear mixer device with a radiation of a referenced frequency. This technique, commonly used in telecommunications and astronomy for detecting and analyzing weak signals, also represents a very convenient way to detect terahertz (THz) radiations. Indeed, heterodyne detection allows the use of conventional microwaves systems (such as spectrum analyzers) and simplifies the signal postprocessing by down-converting the high-frequency (HF) radiation f_{RF} (usually named RF signal) into a signal with an intermediate frequency (IF) f_{IF} falling into the microwave range by the help of an already known radiation [local oscillator (LO)] f_{LO} using the relation: $f_{IF} = \|f_{RF} - f_{LO}\|$ [3]. The state-of-the-art electronic components for direct or heterodyne detections of an HF radiation are achieved by Schottky diodes [4]–[7]. Since these components are based on vertical transport, they require advanced materials, challenging fabrication processes, and critical technology aspects (air bridge to connect the anode introduces more complexity to the fabrication procedure and related parasitic elements) to operate at THz frequencies. More than the mainstream technologies, such as Schottky diodes, the emerging plasma-based detectors [8] also represent a promising alternative for future developments of THz mixers. Based on a different concept, the asymmetric nanodiodes have been proposed to obtain planar devices with nonlinear, diodelike, current–voltage (I–V) characteristic [9]. Moreover, the use of high-mobility semiconductors, such as InGaAs [10] or InAs [11], can improve the cutoff frequency of these nanochannels, thus reaching the THz range at room temperature. However, it should also be possible to achieve THz operations with more robust materials, such as GaN. Even if the use of unipolar GaN nanochannels as THz detectors [12] or mixers [13] is fairly new, it presents a lot of room for improvements to make them competitive with a Schottky technology. In a previous paper, through a systematic numerical study based on Monte Carlo (MC) simulations, we have presented the performances of such GaN nanodiodes as direct and heterodyne detectors in the 0.30-THz frequency range [13]. The aim of this paper is to present, over a wider
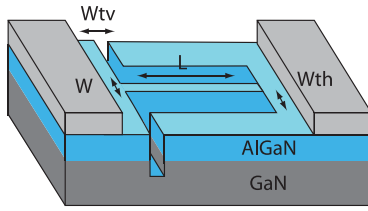
Fig. 1. 2-DEG unipolar nanochannels with a broken symmetry geometry. W and L stand for the channel width and length, and W_{th} and W_{tv} are the widths of the horizontal and vertical trenches, respectively.

Fig. 2. Direct detection setup using the 0.3-THz range source.

frequency range, a systematic experimental study of the performances of GaN nanochannels as direct and heterodyne detectors with particular attention to their dependence on geometry, bias conditions, and frequency of operation. In particular, we show for the first time that GaN nanochannels can be used to detect a radiation at such HFs as 0.69 THz. This paper is organized as follows. Section II introduces the geometries of the different GaN nonlinear nanochannels, the experimental setups, and the MC model. Their performance at frequencies not reported so far (0.64–0.69 THz) is presented in Section III-A and extended to a heterodyne configuration in Section III-B. Finally, the conclusions are given in Section IV.

II. EXPERIMENTAL DETAILS

A. Samples Description

The samples used are based on two dimensional Electron Gas unipolar nanochannels with a broken symmetry created by etching in the AlGaN/GaN heterojunction two symmetrical L-shaped trenches (see Fig. 1 and [12] for technological details). Three geometrical configurations with $L/W =$ 500/500 nm, $L/W = 500/750$ nm, and $L/W = 1000/750$ nm have been tested, where L and W stand for the channels length and width, respectively. Vertical and horizontal trenches are $W_{tv} = 100$ nm and $W_{th} = 50$ nm, respectively. To reduce the impedance of our nanodevices, 32 nanochannels were disposed in parallel without the need of any interconnection. In this way, the extrinsic parasitic elements can be limited, and this is an important feature at these frequencies. We emphasize that the simplicity of the technological process used for the fabrication of these nanodiodes is remarkable, since it only involves the etching of insulating recess lines on a semiconductor surface. Another key aspect of these nanodevices is their planar geometry, which provides the important advantages for the free-space radiation coupling over the traditional diodes (a Schottky barrier) used in current THz systems. In order to use these devices in a free-space configuration, planar bow-tie THz antennas were monolithically integrated with the devices. The bow-ties antennas have been designed to be very broadband, at least from 200 to 700 GHz to be compatible with self-switching devices. Each group of SSD devices was integrated at antenna feed-point, and dc line is feeding each bow-tie ends. The planar design of these antennas enables an SSD array configuration. The use of a large Si lens or an array of Si lenses could also enhance the performances, but for that a dedicated Si-lens array would be required and each signal (LO + RF) would have to be spatially overlapped to feed the mixer.
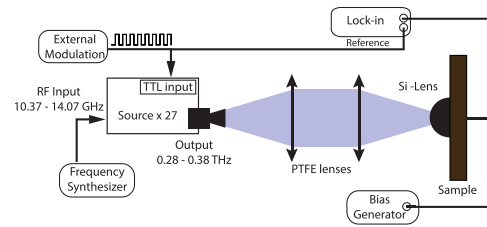
B. Experimental Setups

1) Direct Detection: To highlight the ability of these devices to detect a THz radiation, we have used two electronic sources from Virginia Diodes Inc. (VDI) to cover a large frequency range in experiments. One is a VDI-AMC-S222 tunable from 0.28 to 0.38 THz, and the other is a VDI-AMC-381 tunable from 0.64 to 0.69 THz (Fig. 2). As this kind of electronic sources is composed of a multiplication chain, the measurement frequency points have been verified to be spurious free (e.g., monochromatic signal). At each frequency point, the sources output power was first calibrated using a VDI Erickson PM4 calorimeter matched with a WR10 waveguide load as input. Since we are measuring signals above this waveguide band (59 GHz), adaptation is made by inserting a linear waveguide taper between the source output and the meter input. For the 0.30-THz range source, we used a WR2.8 waveguide taper and measured a power that varies between 0.6 and 1 mW according to the frequency. For the 0.65-THz range source, we used a WR1.2 waveguide taper and measured a power that varies between 1 and 1.3 mW according to the frequency. The RF input of the source is connected using a coaxial cable with subminiature version A (SMA) connectors to a frequency synthesizer Anritsu MG 3692B type, which delivers the microwave signal. This latter will be multiplied by the source. The THz signal is modulated at 1-kHz frequency by an external modulation using an Agilent 33210A function generator connected to the Transistor-Transistor logic input of the source using a coaxial cable with Bayonet Neill–Concelman (BNC) connectors. First, the beam is collimated using a planoconvex polytetrafluoroethylene (PTFE) optical lens of 5-cm diameter and 10-cm focal, and then, it is focused on the sample by another PTFE lens with the same characteristics. Finally, a silicon hemispherical lens of a 6-mm diameter is placed at the rear side of our sample to improve the focalization on each device, to reduce the free-space coupling losses, and to limit interferences inside the Si-bulk layer. The sample is mounted on an FR4-holder, especially designed for 50-Ω impedance matching in the 20-GHz frequency range. The antennas of the devices are connected through gold microbon dings to printed HF lines. The induced photo-voltage is measured using a Signal Recovery 7265 digital signal processing lock-in amplifier, and the dc signal is averaged for each measurement to limit the noise effects. The biasing of the sample is done by a current supplier Keithley type connected to the device by a coaxial cable with BNC connectors.
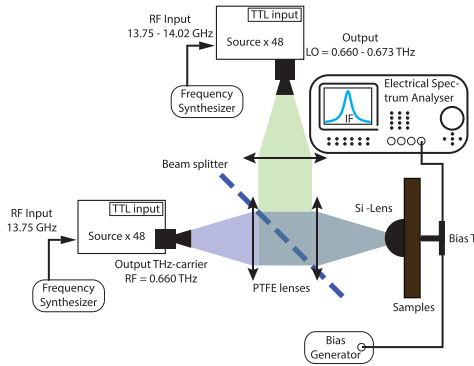
Fig. 3. Heterodyne detection setup using two 0.65-THz range sources.

2) Heterodyne Detection: After ascertaining, using direct configuration, that a device is able to detect a THz radiation, we have studied his ability to mix two THz radiations by modifying the direct detection setup (Fig. 3). To perform heterodyne detection in the 0.30-THz range, we used in addition to the THz source VDI-AMC-S222 type another THz source VDI-AMC-S163 type. This latter has a multiplication factor of 18 and covers the frequency range between 0.22 and 0.32 THz. Its measurement frequency points have been verified to be spurious free and at each frequency point, its output power was calibrated using the VDI Erickson PM4 calorimeter and a WR3.4 linear waveguide taper. We measured a power that varies between 0.6 and 1.6 mW according to the frequency. This source acts as RF frequency provider and is fixed at 0.29 THz, and the second source acts as the LO and its frequency varies between 0.29 and 0.33 THz. To perform heterodyne detection in the 0.65-THz range, we used two identical VDI-AMC-381 THz sources, as shown in Fig. 3. The former one is fixed at 0.66 THz and used as the RF signal, and the second one acts as the LO and its frequency varies between 0.66 and 0.69 THz. These two radiations are collimated and focused using PTFE lenses, whereas a polyethylene terephthalate beam splitter helps to spatially superimpose the two radiations. The Si-lens is still used. A bias-tee, with a bandpass of 50 MHz–26 GHz, is connected to the SMA connectors of the holder in order to provide the dc-bias to the devices (fed by a dc-current source) and to measure the IF, with the help of a Rohde & Schwartz FSU electrical spectrum analyzer. In those experiments, the IF can be measured up to 40 GHz due to the limitation of our spectrum analyzer. In all cases, the experiments were performed in free-space and room temperature configurations. In order to understand the physical mechanisms and to optimize the performances of the devices for broadband direct detection (in terms of responsivity) and mixing (in terms of output power), a semiclassical MC simulation self-consistently coupled with a Poisson solver is used as previously explained in [13].

III. RESULTS AND DISCUSSION

A. Direct Detection

Since for direct detectors, the electrical rectification of an incident electromagnetic radiation is realized through the nonlinearities of the I–V characteristic, we have plotted in Fig. 4, the I–V characteristic of 32 nanochannels with
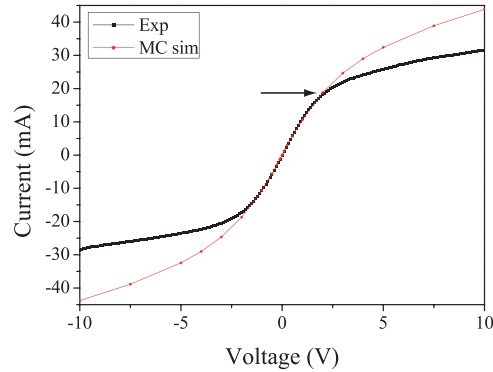

Fig. 4. Comparison between experimental I–V characteristic of 32 nanochannels with $L/W = 500/500$ nm (black line and squares) and MC simulation (red line and dots).
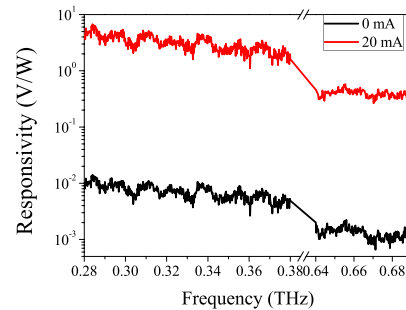

Fig. 5. Experimental responsivity in V/W measured between 0.28 and 0.69 THz, by an array of 32 nanochannels with $L/W = 500/500$ nm, with 0- and 20-mA bias currents.

$L/W = 500/500$ nm. The black curve was experimentally obtained, whereas the red one results from MC simulations. The agreement between MC and measurements is very good in the low bias region showing as well the expected dependence with W and L. However, some discrepancies appear at higher biases. We attribute the differences in the saturation regime to surface charge effects. These discrepancies at the dc level are responsible, latter in this paper, of some differences for the direct and heterodyne detections between MC and experiments.

In order to relate the effect of the bias current on the detector's performances, Fig. 5 shows the measured responsivity between 0.28 and 0.69 THz of an array of 32 nanochannels with $L/W = 500/500$ nm. The plotted responsivities are directly calculated as the ratio between the measured dc signal and the power of the source. Using a current of 20 mA, we clearly observe a responsivity increase of three orders of magnitude, while its frequency dependence remains the same.

To better understand this behavior, we have studied in two frequency ranges (0.29 and 0.66 THz) the responsivity dependence with the current and compared it with the theoretical matched responsivity. The latter is equal to $1/2R_0\gamma$, where R_0 is the zero-bias resistance and γ is the curvature coefficient defined as $\gamma = (d^2I/dV^2)/(dI/dV)$ [14], [15].

Fig. 6 shows a very good agreement—for both frequency ranges—between the current dependence of the responsivity and that of the curvature coefficient. The application of
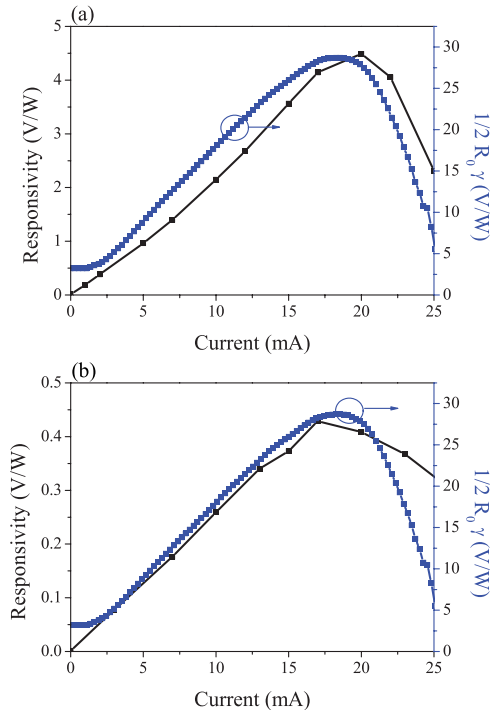
Fig. 6. Experimental responsivity in V/W and $I-V$ curvature versus current at (a) 0.29 and (b) 0.66 THz of an array of 32 nanochannels with $L/W = 500/500$ nm.

Fig. 7. (a) Experimental responsivity in V/W measured between 0.28 and 0.69 THz, by three arrays of 32 nanochannels with different lengths and widths, with 10-mA bias current. (b) MC simulated intrinsic responsivities for the same devices.

an external current leads to higher values of the curvature coefficient and, therefore, to a higher voltage responsivity with an almost constant signal-to-noise ratio $S/N = 12 \pm 1$ in the 0.30-THz range and $S/N = 2.9 \pm 0.3$ in the 0.65-THz range. We notice that the maximum nonlinearity of the $I-V$ characteristic of our device is situated between 17 and 20 mA that is just in the knee of the $I-V$ curve of the nanochannel (indicated by an arrow in Fig. 4), as expected from the well-known link between the RF detection and the nonlinearity of the $I-V$ curve.

Fig. 7(a) shows the responsivities measured between 0.28 and 0.69 THz in three arrays of 32 nanochannels each with different values of L/W and with the same bias current of 10 mA. Fig. 7 shows how reducing the width from 750 down to 500 nm significantly enhances the responsivity up to almost 2 V/W at low frequency, as a result of more prominent surface effects that increase the nonlinearity of the $I-V$ characteristics. On the other hand, the length of the devices hardly affects the value of the responsivity. An important frequency roll-off is observed in all the cases (~20 dB/decade), regardless of the channel geometry, but a strong cutoff is not clearly evidenced by the measurements. Measurements of the beam intensity at 0.30 and 0.65 THz have been performed using a power-meter placed: 1) at the output of the source and 2) at the place where the sample is located. These measurements have allowed us to attribute this frequency dependence mainly to an increase of the optical losses at HF. This is also confirmed because of the MC results shown in Fig. 7(b). The frequency roll-off of these results, which do not consider the optical losses, is much lower (between 2 and 4 dB/decade), with a slightly more pronounced
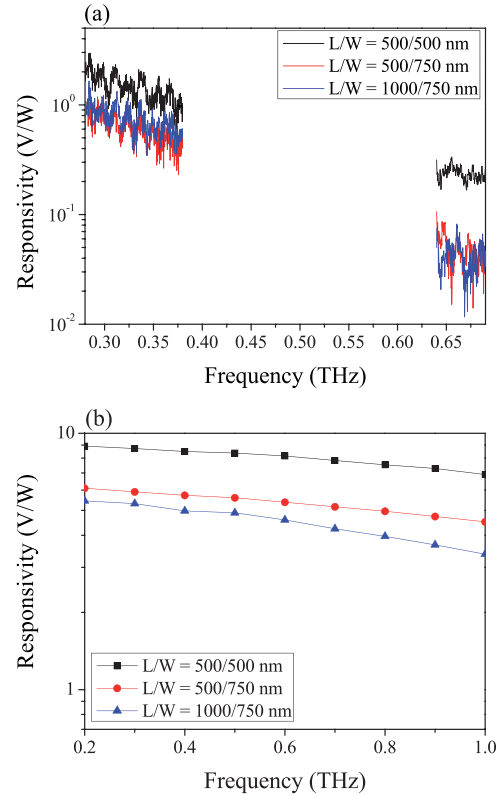
roll-off in the case of $L = 1000$ nm (independently of the width of the channel). A good compromise between length and width is found for $W = 500$ nm and $L = 500$ nm, providing an experimental responsivity above 0.2 V/W up to almost 0.69 THz. At 0.30 THz, these experiments made in a free-space configuration provide a responsivity of ~2 V/W, while the result of MC simulations in guided configuration (on-wafer) is 9 V/W. This comparison allows to estimate the optical losses induced by the coupling of the THz radiation with the device (THz focusing, PTFE and Si lenses, and wave propagation in free space) to be about 6.5 dB at low frequency. However, since we did not perform any data normalization related to the beam spot and the device sizes (which is very difficult to estimate and originates a lot of uncertainty), the real responsivities are probably higher than those reported. Moreover, our maximum detection frequency of 0.69 THz may not represent the upper operational limit of our devices, since as shown by MC simulations, these devices could still be used at frequencies above 1 THz.

B. Heterodyne Detection

The IF power as a function of frequency is presented in Fig. 8 for the RF and LO signals falling into the 0.30-THz range and 0.65-THz range for an array of 32 nanochannels with $L/W = 500/500$ nm for different values of the current. In both cases, a strong attenuation around 13 GHz is observed. This effect cannot be attributed to the cutoff frequency of
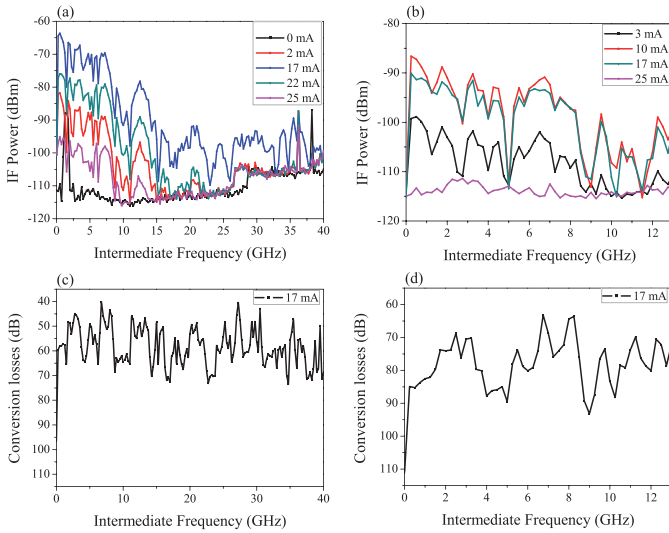
Fig. 8. Experimental IF power measured on a device with $L/W = 500/500$ nm, for different currents, with RF and LO belonging to the frequency ranges (a) 0.30 and (b) 0.65 THz. (c) and (d) Corresponding CLs for $I = 17$ mA.
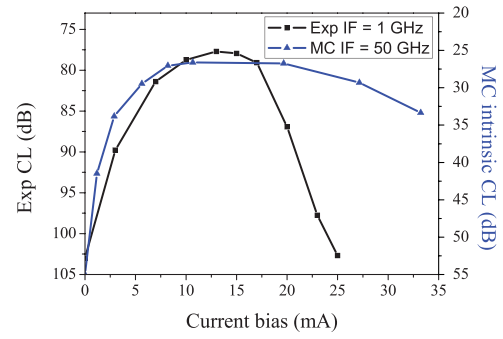

Fig. 9. Experimental power versus current of an IF = 1 GHz and MC intrinsic CLs for an IF = 50-GHz power versus bias current. In this case, a single nanochannel with $L/W = 500/500$ nm is simulated. The RF and LO signals belong to the 0.65-THz range.
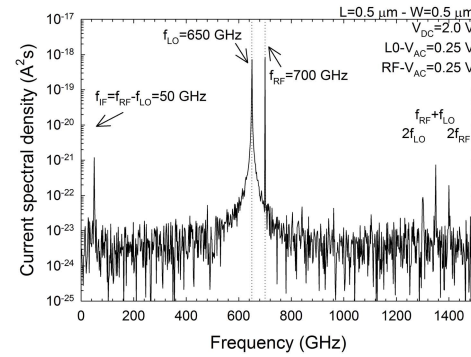

Fig. 10. MC simulated spectra of the current when the frequency of the LO and RF signals are 650 and 700 GHz, respectively, and the bias conditions are VDC = 2 V. In this case, a single nanochannel is simulated with $L/W = 500/500$ nm.

our device. Indeed, the important figures of merit to be considered are the conversion losses (CLs) of our mixer. These have been determined as the ratio of the power at the IF frequency to the power at the RF frequency subtracting the losses induced by connecting elements and HF lines that were simulated using CST microwave studio and present a cutoff frequency around 13 GHz. Consequently, the CL can be plotted according to the IF [Fig. 8(c) and (d)] at 0.30- and 0.65-THz ranges, respectively, for the best bias conditions of $I = 17$ mA. The CLs of the whole integrated device are 58 ± 2 dB at 0.30-THz range and increase by an additional 20 dB at higher frequencies to achieve 78 ± 3 dB at 0.65-THz range. Since CLs are mainly constant in a frequency range (e.g., 0.30 or 0.65 THz), one can conclude that the bandwidth of our mixer is at least of 40 GHz, i.e., the frequency limit of our electrical spectrum analyzer. These values do not represent the intrinsic CL of the devices, since, as for the responsivity measurements, the losses due to radiation coupling with the antenna (especially in the 0.65-THz frequency range) and bondings wires are difficult to estimate experimentally. Using the same method, CL has been calculated for each current, and the results for an IF of 1 GHz (while RF and LO belong to the 0.65-THz range) are plotted in Fig. 9. These results are then compared with the intrinsic CL obtained by an MC simulation done on a single nanochannel with $L/W = 500/500$ nm. Notice that the simulation has been performed for an IF of 50 GHz instead of 1 GHz to decrease the calculation time (and providing the same result, since it is MC IF power is constant below 100 GHz [13]). Fig. 9 shows good agreement between experimental and MC simulation results until a bias current of 17 mA. The disagreement after this biasing point is due to discrepancies between experimental and MC I–V characteristics (Fig. 4). For current lower than 17 mA, by subtracting the intrinsic 27-dB losses calculated by the MC simulation to the

experimental 78-dB losses, we can deduce that the experimental setup (THz focusing, PTFE and Si lenses, and wave propagation in free space) and the device integration (bondings and contacts) introduce the additional losses of ~51 dB.

In Fig. 8(c) and (d), we have estimated that the IF bandwidth of our mixer is at least 40 GHz, which is the limitation provided by our instruments. To confirm this estimation, Fig. 10 highlights the current spectral density calculated for a single nanochannel with $L/W = 500/500$ nm. First, Fig. 10 shows an IF bandwidth up to 50 GHz, since the LO frequency was chosen at 0.65 THz and the RF was chosen at 0.70 THz. Second, the simulated device demonstrates no intrinsic frequency limitation up to 1.35 THz, since a peak corresponding to the upconversion case and with the same order of magnitude as the IF peak is obtained at the frequency $f_{UP} = f_{RF} + f_{LO} = 1.35$ THz.

Finally, another figure of merit of our mixer is studied: the conversion compression, e.g., the maximum RF input power for which the mixer will provide linear operation in terms of constant CL. Fig. 11(a) shows the measurements of the IF output power dependence on the RF input power, whereas Fig. 11(b) presents the corresponding MC simulation results. From experiments, the RF power—measured at the devices top and after all optical elements—varies from -4 to -2.13 dBm. Outside these limits, the power of the RF source is
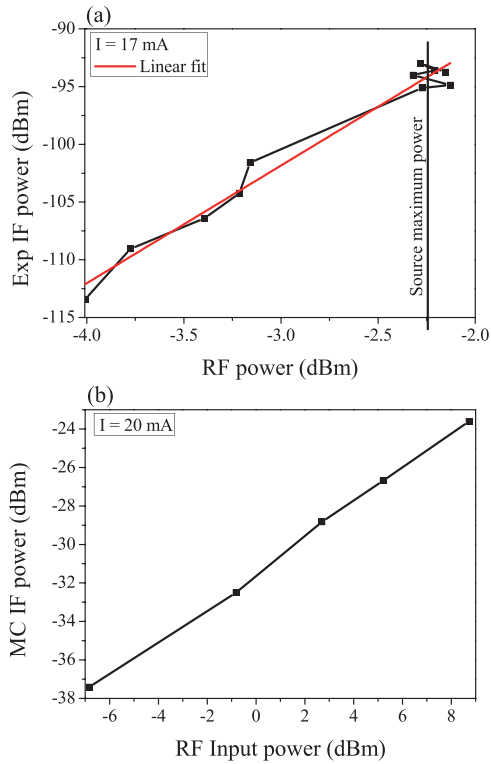
Fig. 11. (a) RF = 0.660 THz and LO = 0.661 THz, experimental IF power versus RF input power measured with an array of 32 nanochannels with $L/W = 500/500$ nm and with a current bias of 17 mA. Straight line: linear fit of the experimental measurements. (b) RF = 0.70 THz and LO = 0.65 THz, MC simulation of the IF power versus RF input power done on the same device with a current bias of 20 mA.

either OFF or reaches its maximum value. In both experimental and MC cases, a linear dependence is observed. From the experimental point of view, no saturation behavior has been observed up to the maximum available power of -2.13 dBm. However, even MC simulations performed for much higher RF power (up to 9 dBm) did not show any saturation of the IF power. This robust linearity of the heterodyne detector response represents a clear advantage compared with the other THz mixers. The important point is that these GaN-based detectors can handle very high input RF power, so that their practical application as the power detectors of ultrahigh-power submillimeter-wave sources seems feasible.

IV. CONCLUSION

In summary, we have investigated the potentialities of AlGaN-/GaN-based nonlinear nanochannels for THz direct as well as for THz heterodyne detection. Their room temperature good responsivity as direct THz and homodyne detectors up to 0.69 THz has been demonstrated for the first time. By comparison with MC simulations, we have found a good compromise between length and width of the nanochannels in order to optimize their responsivity as well as their frequency roll-off at higher frequencies. The qualitative good agreement between experiments and MC simulations will provide the guidelines for improving the SSD performances at THz frequencies.

The characterization of the nanodevices as THz mixers has permitted to highlight two main figures of merit: 1) CLs of 33 dB at 0.65 THz and 2) a strong linearity of the IF output up to 8 dBm of RF input power. As a consequence, since GaN-based nanodevices could handle very high input RF power without deviation from linear regime, their practical implementation as the mixers of high-power submillimeter-wave sources seems feasible. Moreover, recent studies of similar GaN-based nanodiodes [16] have demonstrated their possibilities as Gunn oscillators that could be employed as the active elements of THz emitters. As a consequence, the good performances of GaN nanochannels demonstrated in this paper as the detectors of submillimeter-wave signals as well as their planar geometry allowing not only the easy integration of antennas for a better free-space coupling but also a flexibility in the design for an optimum thermal dissipation and reduction of parasitic effects open the possibility to develop a fully integrated emitter/detector submillimeter-wave system working at room temperature. Besides, this SSD technology is compatible with a power amplifier association on the same dice (adjustment of the conversion gain). It means for heterodyne detection, to process on the same epilayer (heterostructure AlGaN/GaN on a Si substrate) an IF amplifier and an SSD heterodyne mixer. This solution is very promising seeing the low cost solution and the mounting simplification.

REFERENCES

[1] A. Rakshit and A. Chatterjee, "A microcontroller-based compensated optical proximity detector employing the switching-mode synchronous detection technique," *Meas. Sci. Technol.*, vol. 23, no. 3, p. 035102, 2012.

[2] J. Kumar and R. Mehra, "Costas loop implementation for synchronous detection of carrier in radio receiver," in *Proc. Int. Conf. Adv. Comput., Commun. Netw.*, 2011, pp. 975–980.

[3] M. C. Teich, "The physics of heterodyne detection in the far-infrared: Transition from electric-field to photon-absorption detection in a simple system," *Heterodyne Syst. Technol.*, vol. 100, pp. 1–10, Mar. 1980.

[4] H.-W. Hübers, "Terahertz heterodyne receivers," *IEEE J. Sel. Topics Quantum Electron.*, vol. 14, no. 12, pp. 378–391, Mar./Apr. 2008.

[5] H. Kazemi *et al.*, "Ultra sensitive ErAs/InAlGaAs direct detectors for millimeter wave and THz imaging applications," in *Proc. IEEE/MTT-S Int. Microw. Symp.*, Jun. 2007, pp. 1367–1370.

[6] O. Cojocari *et al.*, "A new structural approach for uniform sub-micrometer anode metallization of planar THz Schottky components," *Semicond. Sci. Technol.*, vol. 19, no. 3, pp. 537–542, 2004.

[7] A. Semenov, O. Cojocari, H.-W. Hübers, F. Song, A. Klushin, and A.-S. Müller, "Application of zero-bias quasi-optical Schottky-diode detectors for monitoring short-pulse and weak terahertz radiation," *IEEE Electron Device Lett.*, vol. 31, no. 7, pp. 674–676, Jul. 2010.

[8] D. Glaab, S. Boppel, A. Lisauskas, U. Pfeiffer, E. Öjefors, and H. G. Roskos, "Terahertz heterodyne detection with silicon field-effect transistors," *Appl. Phys. Lett.*, vol. 96, no. 4, p. 042106, 2010. [Online]. Available: http://scitation.aip.org/content/aip/journal/apl/96/4/10.1063/1.3292016

[9] A. M. Song, M. Missous, P. Omling, A. R. Peaker, L. Samuelson, and W. Seifert, "Unidirectional electron flow in a nanometer-scale semiconductor channel: A self-switching device," *Appl. Phys. Lett.*, vol. 83, no. 9, pp. 1881–1883, 2003.

[10] I. Iñiguez-de-la-Torre, H. Rodilla, J. Mateos, D. Pardo, A. M. Song, and T. González, "Terahertz tunable detection in self-switching diodes based on high mobility semiconductors: InGaAs, InAs and InSb," *J. Phys., Conf. Ser.*, vol. 193, no. 1, p. 012082, 2009.

[11] A. Westlund *et al.*, "Optimization and small-signal modeling of zero-bias InAs self-switching diode detectors," *Solid-State Electron.*, vol. 104, pp. 79–85, Feb. 2015. [Online]. Available: http://www.sciencedirect.com/science/article/pii/S0038110114002822

[12] P. Sangaré *et al.*, "Experimental demonstration of direct tera-
hertz detection at room-temperature in AlGaN/GaN asymmetric
nanochannels," *J. Appl. Phys.*, vol. 113, no. 3, p. 034305, 2013.
[Online]. Available: http://scitation.aip.org/content/aip/journal/jap/113/
3/10.1063/1.4775406

[13] I. Íñiguez-de-la-Torre *et al.*, "Operation of GaN planar nanodiodes as
THz detectors and mixers," *IEEE Trans. Terahertz Sci. Technol.*, vol. 4,
no. 6, pp. 670–677, Nov. 2014.

[14] A. M. Cowley and H. O. Sorensen, "Quantitative comparison of solid-
state microwave detectors," *IEEE Trans. Microw. Theory Techn.*, vol. 14,
no. 12, pp. 588–602, Dec. 1966.

[15] Q. Zhou, K.-Y. Wong, W. Chen, and K. J. Chen, "Wide-dynamic-range
zero-bias microwave detector using AlGaN/GaN heterojunction field-
effect diode," *IEEE Microw. Wireless Compon. Lett.*, vol. 20, no. 15,
pp. 277–279, May 2010.

[16] A. Íñiguez-de-la-Torre *et al.*, "Searching for THz Gunn oscillations in
GaN planar nanodiodes," *J. Appl. Phys.*, vol. 111, no. 11, p. 113705,
2012.

Luca Varani received the Ph.D. degree in physics
from the University of Modena, Modena, Italy, and
the Ph.D. degree in electronics from the University
of Montpellier, Montpellier, France.

He is currently a Full Professor with the Institute
of Electronics and Systems, University of Montpel-
lier. His current research interests include theoretical
and experimental transport phenomena in semicon-
ductor materials and devices with a special attention
to terahertz frequencies.

Paul Sangaré, photograph and biography not available at the time of
publication.

Carlos Daher was born in Thoum, Lebanon,
in 1986. He is currently pursuing the Ph.D. degree
with the Institute of Electronics and Systems, Uni-
versity of Montpellier, Montpellier, France.

He is involved in the development of new detectors
and emitters of terahertz radiations based on self-
switching nanodevices.

Guillaume Ducournau received the Ph.D. degree
in fiber optic communication systems using DPSK
modulation schemes from the University of Rouen,
Mont-Saint-Aignan, France, in 2005.

He has been an Assistant Professor with the Insti-
tut d'Électronique de Microélectronique et de Nan-
otechnologie, University of Lille 1, Lille, France,
and the Graduate School, Polytech'Lille, Villeneuve
d'Ascq, since 2007.

Jérémie Torres was born in 1977.

He is currently an Associate Professor of the
Institute of Technology of Montpellier with the
University of Montpellier, Montpellier. His research
has been concerned with high-frequency electronics
and transport in semiconductor materials and devices
for generation, detection, and applications of tera-
hertz radiations. He has authored and co-authored
about 100 scientific articles in refereed journals and
conference proceedings.

Christophe Gaquière received the Ph.D. degree in
electronics from the University of Lille 1, Lille,
France, in 1995.

He is currently a Full Professor with the University
of Lille 1, and carries out his research activity
at the Institut d'Electronique de Microélectronique
et de Nanotechnology. His current research inter-
ests include design, fabrication, characterization, and
modeling of HEMTs and HBT devices.

Ignacio Iñiguez-de-la-Torre was born in Valladolid,
Spain, in 1981.

He is currently a Lecturer with the Electronics
Group, Department of Applied Physics, Univer-
sity of Salamanca, Salamanca, Spain. His current
research interests include development of novel
device concepts for terahertz data processing, detec-
tion, and emission using both narrow and wide
bandgap III–V semiconductors.

Javier Mateos was born in Salamanca, Spain,
in 1970.

He has been with the Department of Applied
Physics, University of Salamanca, Salamanca,
since 1993, where he became an Associate Profes-
sor in 2000. He has authored or co-authored over
100 refereed scientific journal papers and 150 con-
ference contributions. His current research interests
include the study of HEMTs based in both narrow
and wide bandgap semiconductors.

Philippe Nouvel was born in Nimes, France,
in 1975.

He is currently a Project Engineer with the Centre
National de la Recherche Scientifique, University of
Montpellier, France. He is also with the Institute of
Electronics of the South, Montpellier, France, where
he is with the High Frequency Investigation Group.
His current research interests include detection and
generation of terahertz radiations by optoelectronic
systems.

Tomás González was born in Salamanca, Spain,
in 1967.

He has been with the Department of Applied
Physics, University of Salamanca, Salamanca, since
1991, where he is currently a Full Professor of Elec-
tronics. His current research interests include high-
frequency III–V transistors, microscopic modeling
of electronic noise, and development of novel tera-
hertz device concepts based on ballistic transport.